Materials Science & Engineering A 597 (2014) 178–182

Contents lists available at ScienceDirect

Materials Science & Engineering A

journal homepage: www.elsevier.com/locate/msea

Rapid communication

Effects of Gd doping on $Ni_{54}Mn_{25}Ga_{21}$ high-temperature shape memory alloy

Xin Zhang, Jiehe Sui *, Xiaohang Zheng, Zheyi Yang, Wei Cai *

Science and Technology on Materials Performance Evaluation in Space Environment Laboratory, Harbin Institute of Technology, Harbin 150001, China

ARTICLE INFO

Article history:
Received 20 November 2013
Received in revised form
22 December 2013
Accepted 28 December 2013
Available online 8 January 2014

Keywords:
Ni–Mn–Ga alloys
Rare earth Gd doping
Second phase
High-temperature shape memory effect

ABSTRACT

The influence of Gd content on the properties of $Ni_{54}Mn_{25}Ga_{21-x}Gd_x$ alloy was investigated. Proper Gd doping significantly enhanced the mechanical properties. Complete recovery was observed in $Ni_{54}Mn_{25}Ga_{20.9}Gd_{0.1}$ alloy after heating when the pre-strain is less than 10%, while further doping decreased such properties due to the Gd-rich phase formation.

1. Introduction

In recent years, Ni–Mn–Ga shape memory alloy has been widely investigated as ferromagnetic shape memory alloy [1–5]. In addition to the magnetic properties, Ni–Mn–Ga also has many other characteristics. The martensitic transformation temperature (M_s) of Ni–Mn–Ga alloys can be changed in the range from 100 to 450 °C by adjusting the composition due to electron concentration changes [6,7]. Xu et al. reported a shape memory effect (SME) of 6.1% in $Ni_{54}Mn_{25}Ga_{21}$ single crystal with high stability even after 1000 thermal cycles [8]. These qualities make the Ni–Mn–Ga alloy an excellent candidate for high-temperature shape memory alloys (HTSMAs); however, such an alloy is usually too brittle for practical use. Some approaches were adopted to improve its mechanical properties, including grain refinement [9], second phase introduction [10] and fourth element addition [11]. Nevertheless, the mechanical properties and SME of Ni–Mn–Ga polycrystalline alloys were still lower than that of Ni–Mn–Ga single crystal [12,13]. It has been proved that rare earth addition can toughen Ni–Mn–Ga ferromagnetic shape memory alloy. Gao et al. reported that the proper addition of Gd, Dy and Y substituting Ga significantly improved the mechanical properties of the $Ni_{50}Mn_{29}Ga_{21}$ ferromagnetic shape memory alloy [14–16]. So, proper rare earth doping might become an effective method to improve mechanical properties of Ni–Mn–Ga HTSMAs. In this present paper, different amount of Gd is added into $Ni_{54}Mn_{25}Ga_{21}$ HTSMA. The effect of Gd content on microstructure, mechanical properties and SME of $Ni_{54}Mn_{25}Ga_{21-x}Gd_x$ alloys is investigated. The optimal amount of Gd content in these alloys and solubility of Gd in this system are obtained.

2. Experimental

The nominal compositions of the alloys studied were $Ni_{54}Mn_{25}Ga_{21-x}Gd_x$ (x=0, 0.1, 0.3 and 0.5). High purity nickel, manganese, gallium and gadolinium, with a purity level of 99.99%, 99.7%, 99.99% and 99.99%, respectively, were melted in a non-consumed vacuum arc furnace under argon atmosphere. The ingots were remelted six times to ensure homogeneity. The samples were annealed in vacuum quartz tubes at 800 °C for 24 h, and then quenched into ice water.

X-ray diffraction (XRD) measurements were performed by a Rigaku D/max-rB with Cu Kα radiation. The phase transformation temperatures were determined by differential scanning calorimetry (DSC) with heating and cooling rate of 20 °C/min, and the martensitic transformation starting temperatures (M_s) of $Ni_{54}Mn_{25}Ga_{21-x}Gd_x$ (x=0–0.5) are 192 °C, 216 °C, 209 °C and 193 °C. The change of M_s is closely related to the high sensitivity of martensitic transformation temperature to composition of the matrix [7]. The microstructures were surveyed by optical microscopy and transmission electron microscopy (TEM). Thin-foil specimens for TEM observation were mechanically polished to about 100 μm and twinjet electropolished with an electrolyte of nitric acid and methanol (3:7 in volume) at −20 °C, with an electrolytic current of 30 mA. The compression tests were performed at room temperature on an Instron 5569 testing system at

* Corresponding authors. Tel./fax: +86 451 86418649.
E-mail addresses: suijiehe@hit.edu.cn (J. Sui), weicai@hit.edu.cn (W. Cai).

0921-5093/$ - see front matter © 2014 Elsevier B.V. All rights reserved.
http://dx.doi.org/10.1016/j.msea.2013.12.081

a crosshead displacement speed of 0.2 mm/min, and the size of the sample was ∅ 3 mm × 5 mm.

3. Results and discussion

Fig. 1 shows the optical micrographs and XRD patterns of solution-treated $Ni_{54}Mn_{25}Ga_{21-x}Gd_x$ (x=0–0.5) alloys at room temperature. It can be seen that the grain size of Ni–Mn–Ga–Gd alloys decreases with increase in Gd content as shown in Fig. 1(a)-(d). Grain size of $Ni_{54}Mn_{25}Ga_{21}$ alloy is larger than 100 μm, and decreases to 10 μm when the Gd content is up to 0.5 at%. It can be observed that $Ni_{54}Mn_{25}Ga_{21}$ and $Ni_{54}Mn_{25}Ga_{20.9}Gd_{0.1}$ alloys are single-phase. The second phase is formed when Gd content is more than 0.3 at%. A small amount of second phase disperses homogeneously in the matrix of $Ni_{54}Mn_{25}Ga_{20.7}Gd_{0.3}$ alloy. When the Gd content is further increased, the second phase interconnects gradually and tends to gather at the grain boundaries. The solubility of Gd is limited due to the large difference of atom radius between Gd and those elements in the matrix; thus second phase is preferred when the Gd content increases. XRD patterns of $Ni_{54}Mn_{25}Ga_{21-x}Gd_x$ alloys are shown in Fig. 1(e), with six reflection peaks of tetragonal-structured martensite. The positions of the six diffraction peaks of martensite are almost the same even for different Gd contents, which demonstrate that Gd doping does not change the structure of $Ni_{54}Mn_{25}Ga_{21-x}Gd_x$ alloys. No other diffraction peaks could be observed when the Gd content is no more than 0.3 at%, while several additional peaks appear when the Gd content is 0.5 at%, which is rather similar to that of hexagonal $Gd(Ni,Mn)_4Ga$ reported by Cai et al. [14]. It should be noted that when Gd content is 0.3 at%, second phase is observed in Fig. 1(c), while additional peaks are not observed in the X-ray diffraction pattern. This can be attributed to the small fraction of second phase in matrix when Gd content is 0.3 at%.

In order to further confirm the morphology and composition of martensite and second phase in $Ni_{54}Mn_{25}Ga_{21-x}Gd_x$ alloys, TEM observation and EDS were carried out. Fig. 2 shows the TEM images of $Ni_{54}Mn_{25}Ga_{21-x}Gd_x$ (x=0, 0.1, 0.3) alloys and the corresponding diffraction patterns. As shown in Fig. 2(a) and (b), the non-modulated tetragonal martensite in $Ni_{54}Mn_{25}Ga_{21}$ and $Ni_{54}Mn_{25}Ga_{20.9}Gd_{0.1}$ alloys exhibits large stripe-like plates with 1–2 μm in width, and the hair-like stripes can also be seen in the big plate. The martensitic morphology keeps unchanged in $Ni_{54}Mn_{25}Ga_{21}$ and $Ni_{54}Mn_{25}Ga_{20.9}Gd_{0.1}$ alloys. Fig. 2(c) displays a TEM bright field image of $Ni_{54}Mn_{25}Ga_{20.7}Gd_{0.3}$ alloy. Irregular second phase (area B) embedded in plate-like non-modulated tetragonal martensite (area A) which is indexed by Fig. 2(d) is observed, and the width of martensite is narrower than that of monophase alloys. Fig. 2(e) shows the corresponding SAED patterns of area B, which is indexed as $CaCu_5$-type hexagonal structure with the space group of P6/mmm according to the XRD result. Composition of the matrix and second phase of $Ni_{54}Mn_{25}Ga_{21-x}Gd_x$ alloys are listed in Table 1. It can be estimated that (Ni+Mn):Gd:Ga ≈ 4:1:1 (at%) in the second phase of $Ni_{54}Mn_{25}Ga_{20.7}Gd_{0.3}$ and $Ni_{54}Mn_{25}Ga_{20.5}Gd_{0.5}$ alloys. Thus, the chemical formula of this phase can be approximately written as $Gd(Ni,Mn)_4Ga$ according to Cai et al. [14]. The second phase is a Gd-rich phase as seen from the above results.

Fig. 3(a) shows the compressive stress–strain curves of $Ni_{54}Mn_{25}Ga_{21-x}Gd_x$ alloys at room temperature. It can be seen that the compressive strength of Ni–Mn–Ga alloy is obviously enhanced by Gd addition. With the increase of Gd content, compressive strength increases significantly. The largest compressive strength is obtained in $Ni_{54}Mn_{25}Ga_{20.5}Gd_{0.5}$ alloy (approximately 1160 MPa), which is about 770 MPa higher than that of $Ni_{54}Mn_{25}Ga_{21}$ alloy. Furthermore, it should be noted that Gd addition improves the compressive ductility of $Ni_{54}Mn_{25}Ga_{21}$ alloy. The compressive strain is increased with the increase of Gd content and reaches a maximum value (approximately 24.6%) in $Ni_{54}Mn_{25}Ga_{20.9}Gd_{0.1}$ alloy, which is similar to that of $Ni_{54}Mn_{25}Ga_{21}$ single crystal [6]. The improvement in mechanical properties is mainly ascribed to refinement strengthening and solid solution strengthening. It is well known that the ductile second phase is beneficial to improve the mechanical properties of Ni–Mn–Ga alloy [12,13]. In order to know whether Gd-rich phase is a ductile phase, an ingot with the same compositions

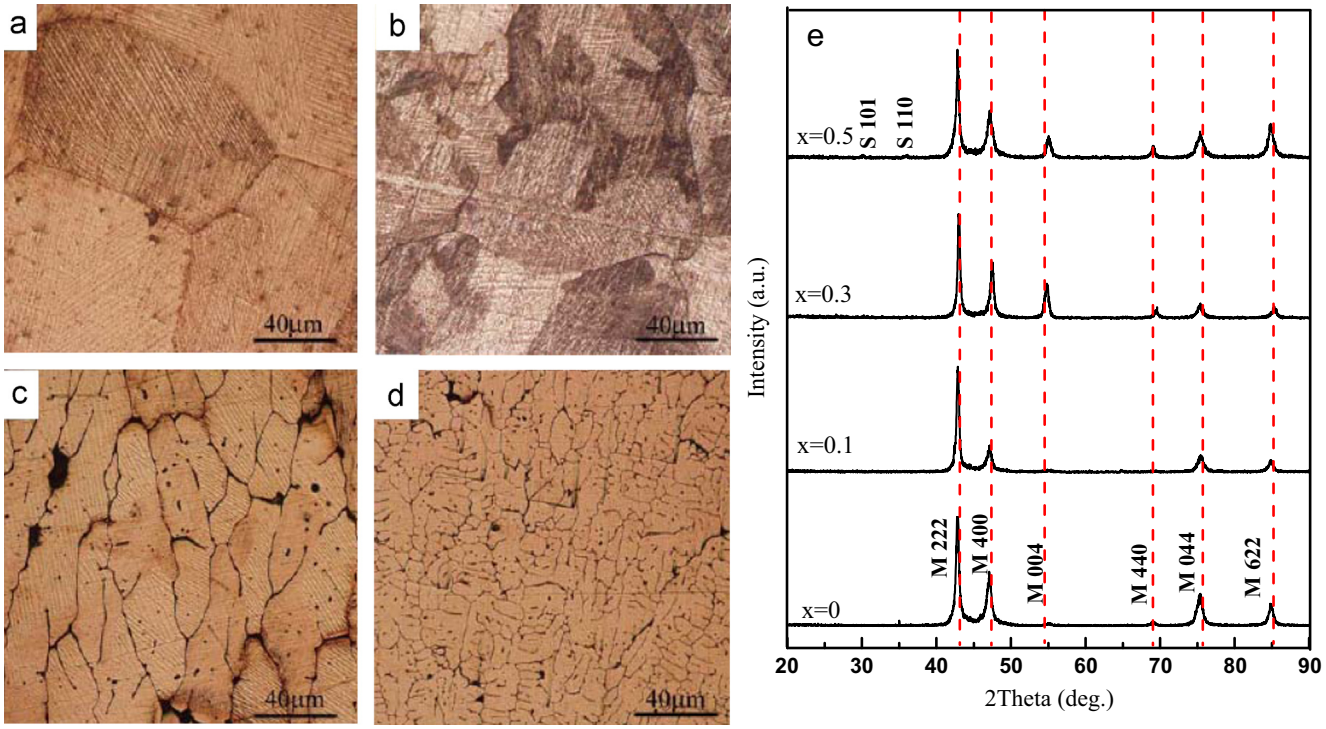

Fig. 1. Optical micrographs of solution treated $Ni_{54}Mn_{25}Ga_{21-x}Gd_x$ alloys. (a) x=0; (b) x=0.1; (c) x=0.3; (d) x=0.5; (e) X-ray diffraction pattern of $Ni_{54}Mn_{25}Ga_{21-x}Gd_x$ alloys at room temperature.